Mutagenesis, 2019, XX, 1–12
doi:10.1093/mutage/gez044
Original Manuscript
Advance Access publication 9 December 2019

OXFORD

Original Manuscript

Effect of 2-acetylaminofluorene and its genotoxic metabolites on DNA adduct formation and DNA damage in 3D reconstructed human skin tissue models

Thomas R. Downs[1], Volker M. Arlt[2,3,4,], Brenda C. Barnett[5], Ryan Posgai[1] and Stefan Pfuhler[1,*]

[1]Procter & Gamble, 8700 Mason-Montgomery Road, Mason, OH 45040, USA, [2]Department of Analytical, Environmental and Forensic Sciences, King's College London, 150 Stamford Street, London SE1 9NH, UK, [3]NIHR Health Protection Research Unit in Health Impact of Environmental Hazards, King's College London in Partnership with Public Health England and Imperial College London, 150 Stamford Street, London SE1 9NH, UK, [4]Present address: GAB Consulting GmbH, Toxicology Department, Heinrich-Fuchs-Str. 96, 69126 Heidelberg, Germany and [5] Adecco Staffing, 4520 Cooper Rd Ste 100, Cincinnati, OH 45242, USA

*To whom correspondence should be addressed. Tel: +1 513 622 1163; E-mail: pfuhler.s@pg.com

Received 31 May 2019; Editorial decision 4 November 2019; Accepted 15 November 2019.

Abstract

In vitro genotoxicity assays utilising human skin models are becoming important tools for the safety assessment of chemicals whose primary exposure is via the dermal route. In order to explore metabolic competency and inducibility of CYP450 activating enzymes, 3D reconstructed human skin tissues were topically treated with 2-acetylaminofluorene (2-AAF) and its genotoxic metabolites, *N*-hydroxy-2-acetylaminofluorene (*N*-OH-2-AAF) and *N*-hydroxy-2-aminofluorene (*N*-OH-2-AF), which primarily cause DNA damage by forming DNA adducts. 2-AAF did not increase DNA damage measured in the reconstructed skin micronucleus (RSMN) assay when administered in multiple applications at 24 h intervals but was detected in the skin comet assay in the presence of the DNA polymerase inhibitor aphidicolin (APC). Similarly, no increase was found with *N*-OH-2-AAF in the RSMN assay after multiple treatments whereas a single 3 h exposure to *N*-OH-2-AAF caused a large dose-related increase in the skin comet assay. A significant increase in the RSMN assay was only obtained with the highly reactive *N*-OH-2-AF metabolite after multiple treatments over 72 h, whereas *N*-OH-2-AF caused a strong increase after a single 3 h exposure in the skin comet assay. In support of these results, DNA adduct formation, measured by the ^{32}P-postlabelling assay, was examined. Adduct levels after 2-AAF treatment for 3 h were minimal but increased >10-fold after multiple exposures over 48 h, suggesting that enzyme(s) that metabolise 2-AAF are induced in the skin models. As expected, a single 3 h exposure to *N*-OH-2-AAF and *N*-OH-2-AF resulted in adduct levels that were at least 10-fold greater than those after multiple exposures to 2-AAF despite ~100-fold lower tested concentrations. Our results demonstrate that DNA damage caused by 2-AAF metabolites is more efficiently detected in the skin comet assay than the RSMN assay and after multiple exposures and enzyme induction, 2-AAF-induced DNA damage can be detected in the APC-modified comet assay.

Introduction

In vitro 3D reconstructed skin comet and reconstructed micronucleus (RSMN) assays using human skin tissue models have been developed and validated to follow up on positive results from the current standard *in vitro* genotoxicity test battery (1–4). As a result of restrictions on *in vivo* testing in animals for cosmetic ingredients (REACh Regulation EC No. 1907/2006; EU Cosmetics Directive 2003/15/EC) (5), these *in vitro* genotoxicity assays are increasingly becoming key tools for the safety assessment of chemicals whose primary exposure is via the dermal route (6,7). The use of the 3D reconstructed skin comet and RSMN assays allows for follow up testing for all genotoxicity endpoints (gene mutation, clastogenicity and aneugenicity) and mimic a more realistic exposure route and thus represent a better test model for topically applied ingredients such as cosmetics and many other types of consumer products. Importantly, the reconstructed skin comet and RSMN assays, both individually and together as a test battery, have good sensitivity and accuracy for predicting *in vivo* genotoxic chemicals (S. Pfuhler et. al., submitted) without the high rate of misleading positives previously seen in the standard battery of *in vitro* genotoxicity tests (8,9).

The importance of skin to act not only as a barrier for penetration of xenobiotics but as a metabolic organ is well recognised (10–12). Similar to the liver, skin has the capacity to either activate or detoxify the genotoxic potential of topically applied chemicals (13–16). However, there are pronounced differences in the metabolic profile of skin compared to liver with respect to phase I metabolism, which is more prominent in the liver compared to skin where phase II enzymes are more highly expressed (17–19). These differences could lead to dissimilarities in the genotoxicity profile of chemicals depending on the route of exposure. The metabolic capacity of various 3D reconstructed human skin models in comparison to 2D monolayer culture systems and native human skin has also been studied extensively (11,14,17–23). There is general agreement that the 3D skin models more closely reflect the metabolism in native human skin than 2D monolayer skin cultures and are valuable tools for predicting the genotoxicity hazard potential of topically applied chemicals.

Validation of the reconstructed skin comet and RSMN assays included testing compounds of various chemical classes with known genotoxic and non-genotoxic profiles *in vivo*, including promutagens that are not genotoxic themselves but can be converted into DNA reactive metabolites. As an example, 2-acetylaminofluorene (2-AAF) and the closely related compound, 2-aminofluorene (2-AF) are genotoxic carcinogens that induce systemic tumours in rodents and other mammals in multiple organs, especially in the liver, urinary bladder, ear duct and mammary gland when administered dermally, orally or by intraperitoneal injection (24–30). In regard to skin, some (25,26,31), but not all studies (28,29,32) have shown evidence that 2-AAF and 2-AF are dermal carcinogens in skin painting studies. The incidence of skin tumours is rare compared to other tumours, however, the length and dosing protocol varies considerably in these older studies. In studies employing oral administration of 2-AAF or 2-AF, skin tumours have not been identified (25,27,30,33), although 2-AAF has been shown to act as an initiator and promoter of epidermal carcinogenesis in mice (33).

The carcinogenic effects of 2-AAF and 2-AF *in vivo* show diverse sex, tissue, and species sensitivities due to differing capacities to convert 2-AAF and 2-AF to their genotoxic metabolites (29,34–38). *N*-hydroxy-2-acetylaminofluorene (*N*-OH-2-AAF) and *N*-hydroxy-2-aminofluorene (*N*-OH-2-AF) are the primary proximate genotoxic metabolites of 2-AAF and 2-AF (39–41) and the known metabolic routes involve both CYP1A2 and *N*-acetyltransferase (NAT) pathways (42–44). *N*-OH-2-AAF and *N*-OH-2-AF are subsequently further metabolised by sulphation or *O*-acetylation to form various electrophilic DNA-reactive compounds (see Figure 1) and consequently DNA adducts (34–36). In studies utilising topical dosing, *N*-OH-2-AAF was a potent inducer of skin and systemic tumours (41), even in species that are resistant to the carcinogenic effects of 2-AAF because of a lack of *N*-hydroxylation activity and/or the presence of additional detoxifying pathways (29,45).

In regard to genotoxicity, 2-AAF and 2-AF are known mutagens but have shown positive responses in tests for both mutagenicity and clastogenicity endpoints *in vivo* in tissues with sufficient metabolic capacity for 2-AAF and 2-AF. Similar results have been found *in vitro* in bacteria and rodent and human cell lines after metabolic activation with rat liver S9 or in cells with endogenous metabolic systems for these chemicals (e.g. liver or bladder cells; reviewed in (34,38,46,47)). Humans have a high capacity for enzymatic conversion of 2-AAF to genotoxic metabolites *in vitro* in many tissues (42,48,49) and although there is evidence for metabolism of topically applied 2-AAF in human skin explants, the specific metabolites could not be identified in the respective study due to technical issues (50). Little information on the genotoxic effects of 2-AAF in skin is available, but in validation studies for the comet assay in 3D reconstructed human skin tissues, topical dosing of 2-AAF was shown to significantly increase DNA damage (S. Pfuhler, submitted). In mice, dermal application of 2-AAF resulted in the formation of DNA adducts in skin, liver, lung and kidney, with skin showing the highest levels of adducts after topical dosing. DNA adducts were also found in skin after both oral and subcutaneous dosing of 2-AAF, but to a lesser extent than in the liver, lung and kidney (51). However, the results of other studies indicated that 2-AAF and 2-AF penetrated rat skin relatively unmetabolised (52).

In this study, 3D reconstructed human skin tissues were topically treated with 2-AAF, *N*-OH-2-AAF and *N*-OH-2-AF for various exposure periods to compare the sensitivity of the skin comet assay and RSMN to detect the DNA damage caused by 2-AAF and its metabolites. Since the expected reactive metabolites are known to bind to DNA, DNA adduct formation, measured by the ^{32}P-postlabelling assay, was used as a surrogate to estimate the amount of DNA reactive metabolites generated in the skin tissue models as a function of exposure time and frequency of treatment.

Material and methods

Test compounds

N-OH-2-AAF (CAS No. 53-95-2, >99% purity by HPLC) and *N*-OH-2-AF (CAS No. 53-94-1, >89% purity by NMR) were purchased from MRIGlobal Chemical Carcinogen Repository (Kansas City, MO). 2-AAF (CAS No. 53-96-3, >98% purity by HPLC), methyl methanesulphonate (MMS), benzo[*a*]pyrene (BaP) and mitomycin C (MMC) were purchased from Sigma–Aldrich (Saint Louis, MO).

Skin tissue models

EpiDerm™ skin tissues (EPI-200-MNA) for the RSMN assay were obtained from MatTek Corporation (Ashland, MA) and cultured in 1 ml of new maintenance medium (NMM) at 37°C and 5% CO_2. NMM was replaced just prior to each chemical treatment and also contained cytochalasin B (CytoB; Sigma–Aldrich, Saint Louis, MO; 3 µg/ml) during the treatment periods (3). Phenion® Full-Thickness skin tissues (Phenion®FT) for the skin comet assay were purchased

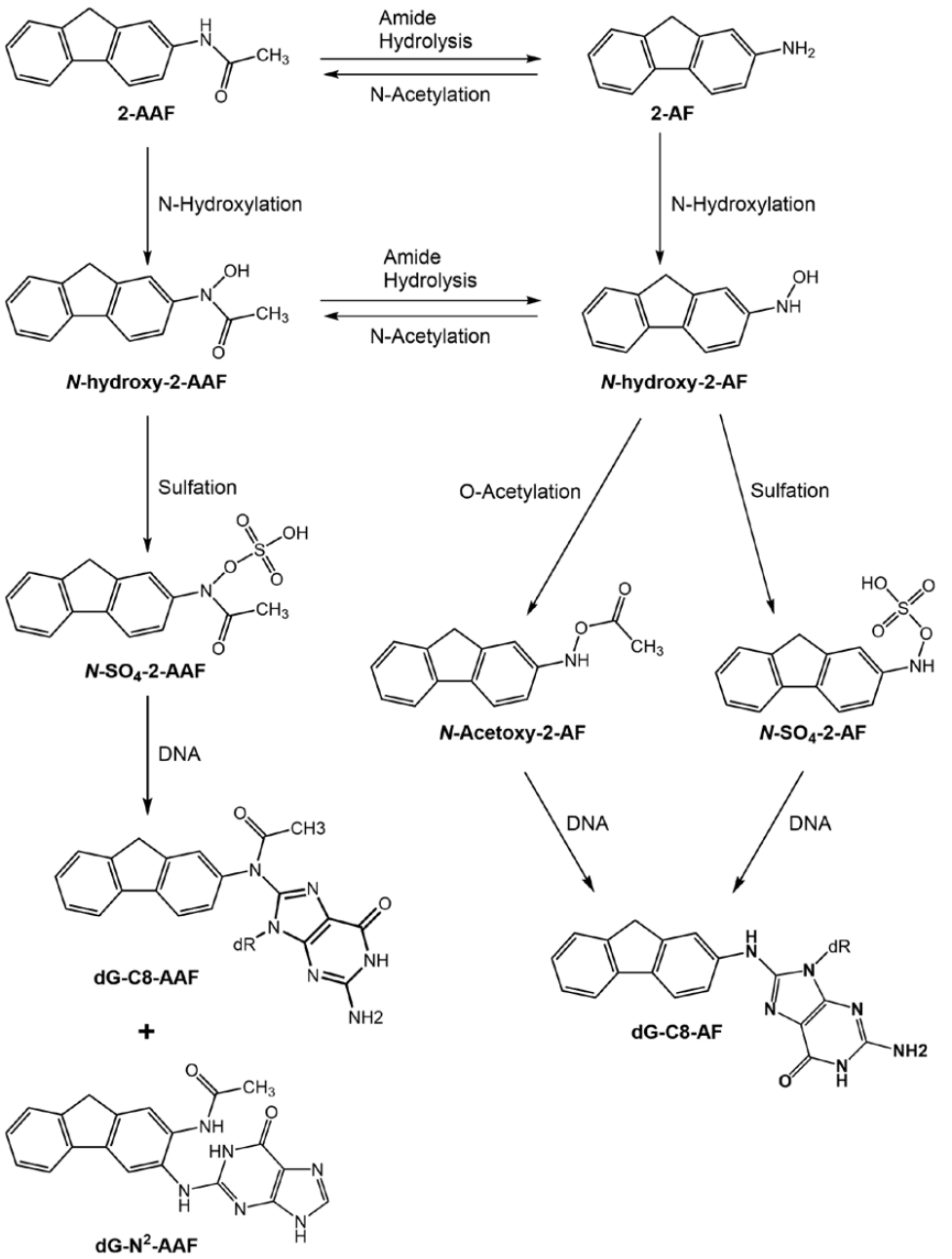

Fig. 1. Metabolism of 2-AAF. *N*-hydroxylation leads to the formation of the reactive metabolite *N*-hydroxy-2-AAF (*N*-OH-2-AAF). Amide hydrolysis and subsequent *N*-hydroxylation lead to formation of the highly reactive metabolite *N*-hydroxy-2-AF (*N*-OH-2-AF). Sulphation or *O*-acetylation of these metabolites leads to the formation of other DNA-reactive compounds as indicated in the scheme.

from Henkel (Düsseldorf, Germany) and cultured in 5 ml air–liquid-interface (ALI) medium at 37°C and 5% CO_2. The medium was refreshed one time after an initial overnight equilibration period just prior to the first chemical treatment (4).

Chemical treatments for RSMN and skin comet assays

For the RSMN assay, chemicals were applied topically to the EpiDerm™ skin tissues in 10 µl (16 µl/cm^2) of acetone using two or three treatments at 24 h intervals over 48 h or 72 h to allow for induction of metabolic enzymes and possible transformation of chemicals (3,17,20). The 72-h (three treatment) protocol has been previously shown to increase the sensitivity of the RSMN assay without affecting the specificity (53). A solvent control (SC) and positive control (PC; MMC 0.05 µg/cm^2, two or three treatments over 48 h or 72 h) were included in each assay.

For the 3D skin comet assay in Phenion®FT skin tissues, chemicals were applied in 25 µl (16 µl/cm^2) of acetone over 48 h. After the initial treatment, chemicals were re-applied at 24 h and 45 h after the first dose. The last treatment (a 3-h exposure) was used to maximise the detection of DNA damage that may be repaired quickly (4). In cases where the reactive 2-AAF metabolites were tested, only one 3 h treatment was used. A SC and PC (MMS; 5 µg/cm^2, one (3 h) treatment at 45 h) were included in each assay. In some experiments, aphidicolin (APC; Sigma–Aldrich, Saint Louis, MO; 5 µg/ml) was added to the medium 4 h before the end of the incubation which has

been shown to increase the sensitivity of the comet assay without affecting the specificity (4,14,54). In the APC experiments, the promutagen BaP (12.5 µg/cm^2, three treatments over 48 h) was used as the PC to demonstrate the effectiveness of APC.

For both the skin comet and RSMN assays, all groups were done in triplicate and all chemicals were prepared fresh just prior to each dosing. The maximum test doses used for each chemical were determined in preliminary experiments considering the thresholds for excessive cytotoxicity in each assay.

RSMN assay procedure

The RSMN assay was conducted according to the protocol described (2,3,55). In brief, at the end of the treatment period, tissues were washed for 5 min in 5 ml Dulbecco's phosphate-buffered saline (w/o Ca^{2+}/Mg^{2+}) (DPBS; Life Technologies, Carlsbad, CA), followed by 15 min in 5 ml DPBS containing EDTA (0.1%), then incubated in 1.5 ml 0.25% trypsin–0.02% EDTA for 15 min at 37°C followed by the addition of 1 ml NMM containing 10% foetal bovine serum. Tissues were detached from the support membrane with forceps and single cell suspensions generated by repeatedly pipetting the medium over the tissues. The viable cell number from each tissue was determined and the remaining cells were centrifuged (100 × *g*) and resuspended in 1 ml of warm (37°C) 0.075 M KCl while mixing gently. After 3 min, 3 ml of cold (4°C) methanol/acetic acid (3:1, v:v) fixative was added and the suspension centrifuged at 100 × *g* for 5 min. The fixation was repeated using 3 ml of cold methanol/acetic acid (40:1, v:v) to minimise salt crystals. A single drop (30–40 µl) of the concentrated cell suspension was pipetted onto two microscope slides, allowed to dry, and then stored at 4°C.

Comet assay procedure

The skin comet assay was performed according to the procedure described (4). Briefly, at the end of the chemical treatment period, the Phenion®FT skin tissues were rinsed with 1 ml DPBS and approximately 25% of each tissue was cut off, snap frozen in liquid nitrogen and stored at −80°C for determining intracellular adenosine triphosphate (ATP) and protein levels. The culture medium was stored at 4°C for assaying adenylate kinase (AK) activity. The remaining tissue was placed on top of 300 µl thermolysin (0.5 mg/ml in 10 mM HEPES, 33 mM KCl, 50 mM NaCl and 7 mM $CaCl_2$, pH 7.2–7.5) in a 12-well plate at 4°C for 2 h, and the dermis and epidermis were separated using forceps. The two layers were transferred separately to 1 ml each cold mincing buffer (20 mM EDTA in Hank's balanced salt solution w/o Ca^{2+}/Mg^{2+}, 10% DMSO, pH 7.5), cut into small pieces (20–30 times) using scissors and filtered through 40 µm strainers (BD Biosciences, Franklin Lakes, NJ). The cells and nuclei were centrifuged (5 min, 250–300 × *g*), the medium decanted, and the pellet resuspended in the residual supernatant. The cells were mixed with 300 µl 0.5% low-melting agarose (SeaPlaque® GTG® Agarose; Lonza, Basel, Switzerland) in DPBS and 75 µl was transferred to three agarose-coated (1%) microscope slides. Slides were covered with coverslips and cooled for 5 min to allow solidification. The coverslips were removed and cells were lysed at 4°C overnight in lysis solution (2.5 M NaCl, 0.1 M Na_2EDTA, 0.01 M Tris, pH 10, 1% Triton X-100 and 10% DMSO). Slides were incubated in cold electrophoresis solution (0.3 M NaOH and 0.001 M Na_2EDTA, pH > 13) for 20 min to allow for DNA unwinding prior to electrophoresis at 4°C for 30 min at 39 V and 450 ± 10 mA with fresh solution in a chamber from Carl Roth (Karlsruhe, Germany, #N610.1). Slides were then neutralised in 0.4 M Tris–HCl, pH 7.5 for 10 min, dehydrated in absolute ethanol for 2–3 min, allowed to dry, and stored at room temperature.

DNA staining and slide analysis

The analysis of comet and RSMN slides was performed based on recently published standards (1,3). In brief, slides were randomised and coded by a separate person so the treatments were blinded to the scorer to prevent evaluator bias. For the RSMN assay, cells were stained with acridine orange (Sigma–Aldrich, Saint Louis, MO; 40 µg/ml in DPBS) for 2–3 min, then rinsed three times with DPBS and a coverslip placed on top. Slides were scored using a fluorescence microscope with a ×40 objective. The % of binucleated (BN) cells was measured in 500 cells/tissue and the % of BN cells with micronuclei (% MN-BN) was determined in 1000 BN cells/tissue.

For the comet assay, nuclei were stained for 15 min with a 1:10 000 dilution of SYBR® Gold (Life Technologies, Carlsbad, CA) in 0.05 M Tris–HCl pH 7.5 and a coverslip placed on top. The tail intensity (% tail DNA; 0–100%) was scored using a fluorescence microscope with a ×20 objective and the Comet Assay IV software (Perceptive Instruments, Suffolk, UK). For each tissue, three slides were analysed, scoring 50 cells per slide (150 cells per tissue) and three tissues per treatment for a total of 450 cells per group.

Cytotoxicity assessment

For the RSMN assay, cytotoxicity was determined by measuring the viable cell count (VCC) and frequency of binucleated cells (% BN). The VCC was determined after differential staining with AO/DAPI using a NucleoCounter NC250 (ChemoMetec A/S, Allerod, Denmark). The BN frequency was measured using a fluorescence microscope after AO staining. The % VCC and % BN for each group were expressed relative to the SC. The thresholds set for excessive cytotoxicity for % VCC and % BN were a 55 ± 5 % reduction as described previously (3) and per the current OECD 487 test guideline for the *in vitro* MN assay (56). If cytotoxicity was observed with both measurements, the more sensitive parameter was used.

For the skin comet assay, cytotoxicity was determined by measuring the AK activity (57) and the intracellular ATP concentration (58). AK was measured using the ToxiLight bioassay kit (Lonza, Basel, Switzerland). For ATP, frozen tissues were homogenised in 1 ml of cold DPBS in a TissueLyzer II (Qiagen, Hilden, Germany) for 5 min at 30 Hz using a 5 mm stainless steel bead. Homogenates were then heated for 5 min at 105°C, transferred to ice and centrifuged at 10 000 × *g* for 2 min. ATP was determined in the supernatants using the ATPlite Kit (Perkin Elmer, Waltham, MA). To normalise for variations in the size of the tissue slices, the protein content was also measured using the Bradford assay (BioRad, Hercules, CA) and ATP levels were expressed as µg ATP/mg protein. The % ATP and % AK were expressed relative to those of the SC. The thresholds set for excessive cytotoxicity were a ≥2-fold increase in AK activity and/or ≥50% decrease in ATP/protein as previously described (4). If cytotoxicity was observed with both measurements, the more sensitive parameter was used.

DNA isolation and DNA adduct analysis

Genomic DNA was isolated from Phenion®FT skin tissues at the end of the chemical treatment period for the determination of DNA adducts. Tissues were rinsed with 1 ml DPBS, cut into 15–20 smaller pieces and transferred to a 2 ml eppendorf tube. Next 1.5 ml of DNAzol (Molecular Research Center Inc., Cincinnati, OH) containing 30 µl of a proteinase K solution (20 mg/ml; Qiagen, Hilden,

Germany) was added and the tubes were placed on a platform rocker (speed 15 rpm) at room temperature for 20 h. The tubes were centrifuged at 10 000 × *g* for 5 min at 4°C, 100% ethanol (0.75 ml) was added to the supernatants and the tubes were mixed slowly by inversion (×20–25). After a 5 min at room temperature, tubes were centrifuged at 2000 × *g* for 5 min at 4°C to pellet the DNA. The supernatants were discarded, 1 ml 75% ethanol was added, and the tubes were mixed by inversion. The tubes were centrifuged at 10 000 × *g* for 2 min, the supernatants discarded, and the pellets washed two additional times. The supernatants were removed, and the DNA was solubilised in 30 µl 10 mM Tris–HCl, 1 mM EDTA, pH 8. Total DNA was measured with a NanoVue™ UV/Visible Spectrophotometer (GE Healthcare Biosciences, Uppsala, Sweden).

DNA adduct formation was measured by the thin-layer chromatography (TLC) ^{32}P-postlabelling assay which was essentially performed as reported (59,60) with minor modifications (see below). For 2-AAF, *N*-OH-2-AAF- and *N*-OH-2-AF-treated samples, DNA adducts were enriched by butanol extraction (61), whereas for BaP-treated samples the nuclease P1 digestion enrichment method was used (62). DNA (4 µg) was digested overnight with micrococcal nuclease (Sigma–Aldrich, Saint Louis, MO; 288 mU/sample) and calf spleen phosphodiesterase (MP Biomedicals, Santa Ana, CA; 1.2 mU/sample), enriched and labelled with 50 µCi [γ-^{32}P]-ATP (Hartmann-Analytic, Braunschweig, Germany; HP601PE). Solvent conditions for TLC on polyethyleneimine-cellulose (Macherey-Nagel, Düren, Germany) were D1, 1.0 M sodium phosphate, pH 6.0; D3, 4 M lithium formate and 7 M urea, pH 3.5 and D4, 0.8 M lithium chloride, 0.5 M Tris and 8.5 M urea, pH 8.0. After chromatography, TLC sheets were scanned using a Packard Instant Imager (Downers Grove, IL) and DNA adduct levels (relative adduct labelling or RAL) were calculated from the adduct counts per minute, the specific activity of [γ-^{32}P]-ATP and the amount of DNA used. Results were expressed as DNA adducts per 10^8 nucleotides.

Data evaluation

For the RSMN, the % MN-BN cells were analysed using a one-sided Fisher's exact test to determine the statistical significance of differences between SC and the chemical treatment groups. A Cochran–Armitage trend test was also used to evaluate the overall dose response. A *P*-value <0.05 was considered a significant increase for both tests (3). For a valid RSMN experiment, the SC group must have a minimum cell yield of 5 × 10^4 cells/tissue, a % BN of at least 25%, and the % MN-BN cells in the SC group is within the acceptable historical range for the laboratory. An average of about 0.1% (range of 0–0.5%) has been obtained across a number of laboratories in the RSMN prevalidation studies. The PC (MMC) must also show a statistically significant increase in the % MN-BN above the SC as previously described (3). A valid dose group must also not exceed the thresholds for excessive cytotoxicity described above.

For the skin comet assay, the raw % tail DNA data were aggregated as follows: for each slide, the median was calculated from the 50 comet scores and the median values were then arcsine square-root transformed to achieve normality and variance homogeneity. For each tissue, the transformed medians of the three slides were averaged and the values for the keratinocytes and fibroblasts were analysed separately (1,4). The comet assay results and DNA adduct levels were analysed using a one-way analysis of variance (ANOVA) or *t*-test when only two groups were compared. In case of a significant difference in the ANOVA, each test chemical treatment group was individually compared to the SC or SC + APC group as appropriate using the one-sided Dunnett test (63) to identify groups showing a significantly ($P < 0.05$) increased response. A significant response in either cell type in the comet assay was considered as a positive response to the test chemical as previously described (4). For a valid experiment in the standard comet assay protocol, the SC had to display ≤20% tail DNA and the PC (MMS) had to show at least a 2-fold increase in % tail DNA compared to SC, as well as an absolute increase in % tail DNA by ≥15 percentage points above the SC. For the APC protocol, the SC + APC had to also display ≤20% tail DNA and the positive control (BaP + APC) had to show an increase in % tail DNA by ≥5% tail DNA above the SC + APC as previously described (4). A valid dose group must also not exceed the thresholds for excessive cytotoxicity described above.

Results

Effect of 2-AAF and metabolites on DNA damage in the RSMN assay

Based on the results by Hu (20) and Wiegand (17) who showed that phase I enzymes in skin tissues and human native skin are clearly induced within 48 h, we topically exposed skin tissues with test chemicals for 48 h to facilitate the conversion of promutagens into DNA reactive mutagens. Treatment of EpiDerm™ skin tissues with 2-AAF two times over a 48-h period at doses up to 140 µg/cm^2, which caused a reduction in % VCC that exceeded the cytotoxicity threshold of a 55 ± 5 % reduction compared to the SC (3,56), did not result in a significant increase in MN formation (Figure 2a). The addition of a third treatment with 2-AAF over 72 h has been demonstrated to increase the sensitivity of the RSMN assay in the EpiDerm™ skin tissues without sacrificing its specificity (53). However, using three doses of 2-AAF up to 96 µg/cm^2 which exceeded the cytotoxicity threshold by % VCC, also did not significantly increase DNA damage in the RSMN assay (Figure 2b). Similarly, two or three treatments with the 2-AAF metabolite, *N*-OH-2-AAF over 48 h or 72 h did not cause a significant increase in DNA damage in the RSMN assay (Figure 2c and d) at doses up to 0.8 µg/cm^2 which exceeded the cytotoxicity threshold by % BN. Two treatments with the highly reactive 2-AAF metabolite, *N*-OH-2-AF over 48 h also did not significantly increase MN formation up to threshold cytotoxic doses of 1.3 µg/cm^2 by % VCC (Figure 2e). A significant change in micronuclei in the RSMN assay was only seen after a third treatment over 72 h with *N*-OH-2-AF ($P < 0.01$) at the two highest doses (0.85 and 1.3 µg/cm^2; Figure 2f) which approached the cytotoxicity threshold for % VCC at the highest dose. In all experiments, treatment of the EpiDerm™ skin tissues with MMC as PC resulted in highly significant increases in MN formation after either two or three treatments over 48 h and 72 h, respectively (Figure 2a–f).

Effect of 2-AAF and metabolites on DNA damage in the skin comet assay

Treatment of Phenion®FT skin tissues with 2-AAF three times over a 48-h period at doses up to 150 µg/cm^2 in two separate experiments resulted in a statistically significant increase in DNA damage compared to the SC group in the comet assay only in the fibroblasts at 75 µg/cm^2 in the second experiment (Figure 3d). Application of the same three-treatment protocol with 2-AAF in the presence of APC, an inhibitor of DNA polymerases α and δ (54), caused a significant increase in the % tail DNA compared to the SC + APC group in the fibroblasts in both experiments at all doses tested (Figure 3b and d). Although the response in the keratinocytes was only statistically significant in one experiment (Figure 3c) at a dose (75 µg/cm^2) that exceeded the % ATP cytotoxicity threshold, the addition of APC consistently increased DNA damage in response to 2-AAF compared to the SC + APC controls in both

experiments in the keratinocytes and fibroblasts (Figure 3a–d). APC alone showed only a small non-significant increase in DNA damage compared to the SC group alone (Figure 3a–d). BaP, used as PC for the APC-modified comet assay protocol, also showed only a small non-significant increase in DNA damage vs the SC group using the standard three-treatment 48 h protocol without APC but exhibited a highly significant increase in DNA damage in the presence of APC in both the keratinocytes and fibroblasts (Figure 3a–d).

In contrast to 2-AAF, a single 3 h treatment of Phenion®FT skin tissues with two genotoxic metabolites of 2-AAF, resulted in highly significant, dose-responsive increases in DNA damage in the comet assay at non-cytotoxic doses. *N*-OH-2-AAF significantly increased the % tail DNA at a dose of 4 µg/cm² in keratinocytes and fibroblasts (Figure 4a–b). The DNA damage caused by treatment with *N*-OH-2-AAF alone at 1 and 4 µg/cm² was further amplified in the presence of APC in both cell types (Figure 4a–b). A single 3 h treatment of Phenion®FT skin tissues with another highly reactive 2-AAF metabolite, *N*-OH-2-AF, showed a robust, dose-responsive increase in DNA damage at doses of 0.25–4 µg/cm² which reached near maximal levels (60–80% tail DNA) at a dose of 1 µg/cm² in the keratinocytes and fibroblasts (Figure 4c–d). In the presence of APC, the DNA damage measured in the comet assay was further amplified and

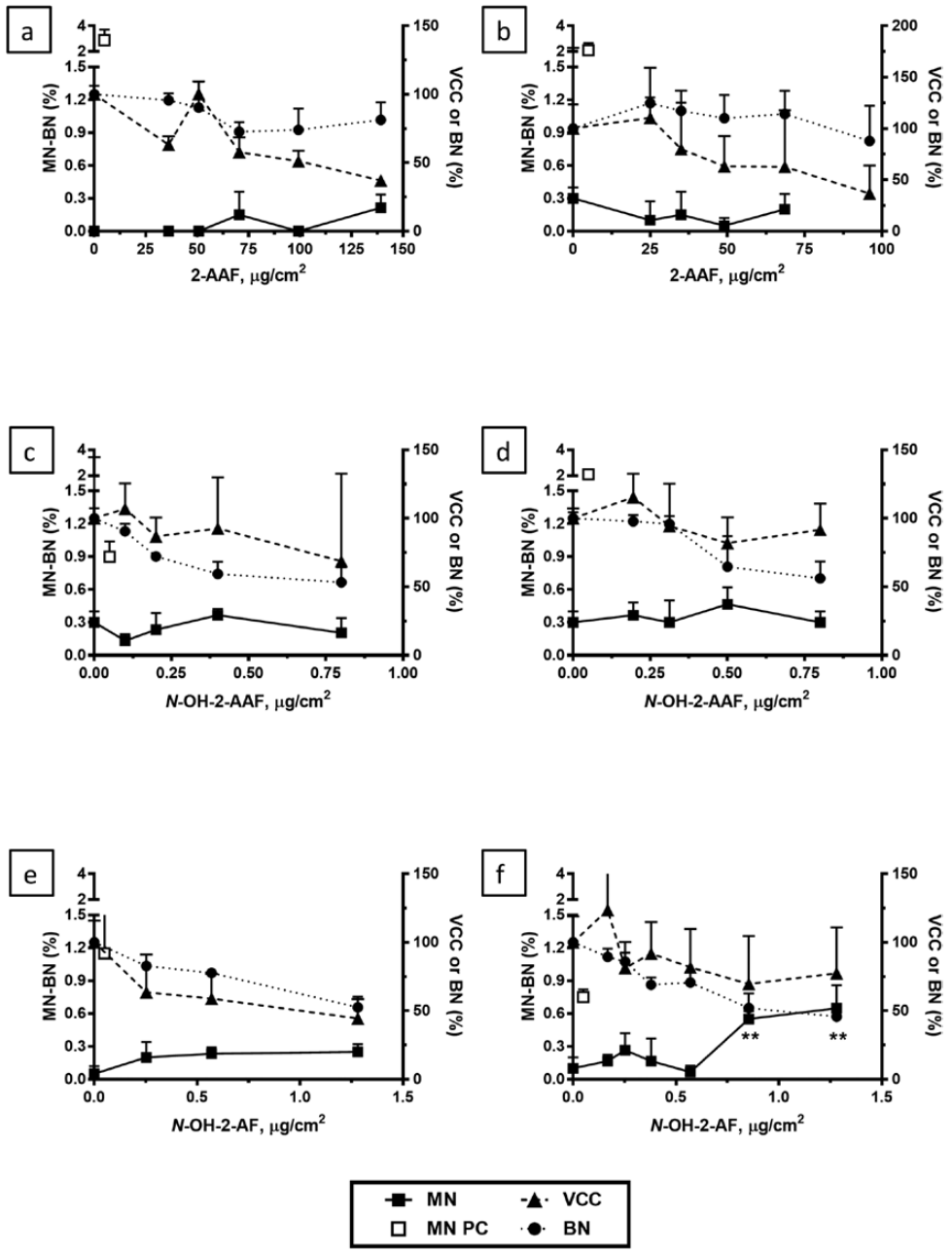

Fig. 2. DNA damage (% MN-BN) measured in the RSMN assay in the Epiderm™ skin model induced by 2-AAF (a, b, upper panels), *N*-OH-2-AAF (c, d, middle panels), and *N*-OH-2-AF (e, f, lower panels). Tissues were treated two or three times at 24 h intervals for all compounds (48 h treatment; a, c, e, left panels and 72 h treatment; b, d, f, right panels). Cytotoxicity measures were % VCC and % BN relative to the solvent controls which were set at 100%. All values ($n = 3$) are mean ± SD. $^{**}P < 0.01$. PC: MMC.

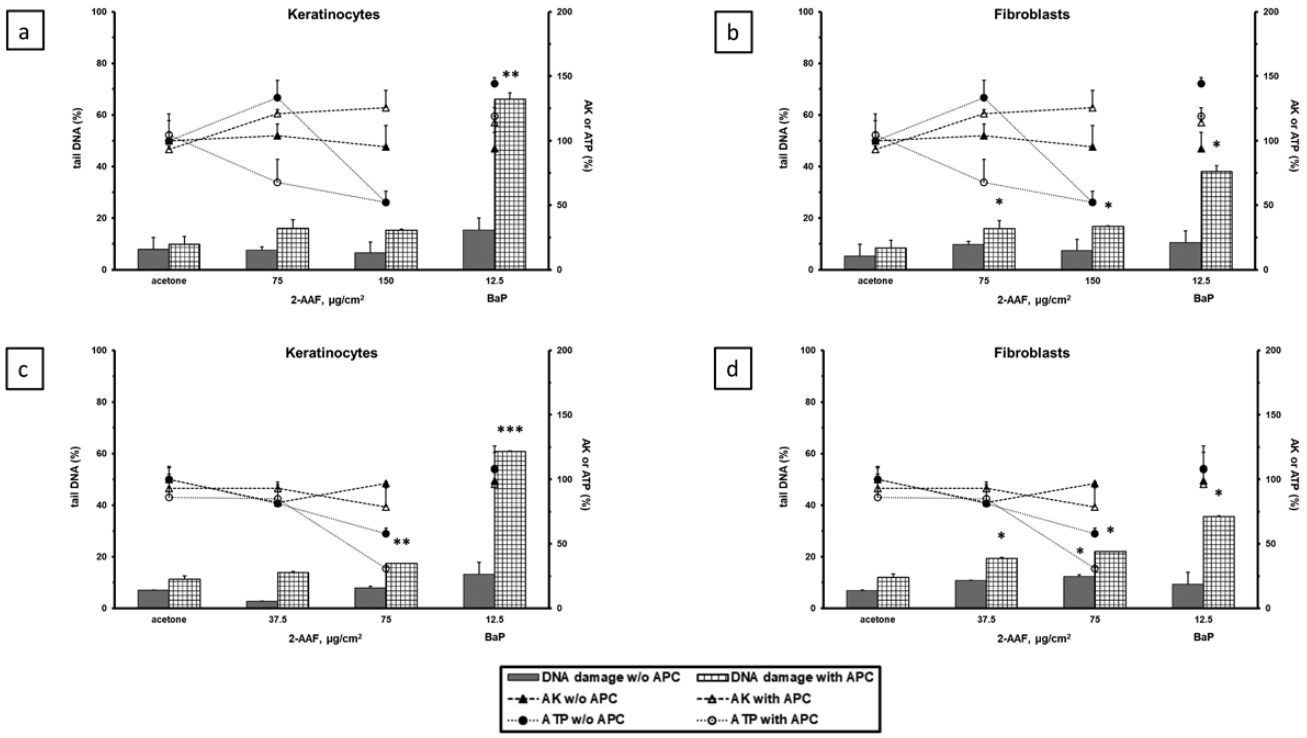

Fig. 3. DNA damage (% tail DNA) measured in the comet assay in the Phenion® FT skin model induced by 2-AAF ± APC in keratinocytes (a, c, left panels) and fibroblasts (b, d, right panels) in two separate experiments. Tissues were treated three times (48, 24 and 3 h) with 2-AAF ± APC. Cytotoxicity measures were % AK release and % ATP content relative to the solvent controls which were set at 100%. All values ($n = 3$) are mean ± SD. $^{*}P < 0.05$, $^{**}P < 0.01$, $^{***}P < 0.001$. PC: BaP.

reached near maximal levels at all three doses of *N*-OH-2-AF in both cell types (Figure 4c–d) in the absence of excessive cytotoxicity. Similar results to those seen in the Phenion®FT skin tissues were also seen in the EpiDerm™ skin tissues in which a single 3 h treatment with *N*-OH-2-AAF at doses ≥2 µg/cm² resulted in a highly significant dose-dependent increase in DNA damage in keratinocytes in the skin comet assay (data not shown).

Effect of 2-AAF and metabolites on DNA adduct formation

Previous studies have shown that 2-AAF is capable of inducing multiple DNA adducts *in vivo* in skin and other tissues which are detectable by TLC ^{32}P-postlabelling (51,64–69). The major DNA adducts previously identified *in vivo* include the non-acetylated adduct *N*-(deoxyguanosin-8-yl)-2-aminofluorene (dG-C8-AF) and two acetylated adducts, *N*-(deoxyguanosin-8-yl)-2-acetylaminofluorene (dG-C8-AAF) and 3-(deoxyguanosin-N^2-yl)-2-acetylaminofluorene (dG-N^2-AAF), respectively (64,65). The DNA adduct pattern induced by 2-AAF, *N*-OH-2-AAF and *N*-OH-2-AF in Phenion®FT skin tissues was similar, consisting of one major DNA adduct spot (Figure 5a–d). As expected, no 2-AAF-related DNA adducts were detectable in the SC group as no exposure had occurred (Figure 5a). It is noteworthy that several minor DNA adduct spots were detectable in *N*-OH-2-AAF-treated tissues (Figure 5c). Although it was beyond the scope of the present study to prove the identity of the DNA adducts detected, based on the adduct profiles observed in previous studies (51,64,66,67), the major spot detected here was tentatively assigned to be the dG-C8-AF adduct. However, as no authentic standards were available, this conclusion has to be treated with caution; also, because experimental conditions (e.g. solvents) used in the present study may not be exactly the same as those used previously. In addition, as the DNA adduct pattern induced by 2-AAF has been shown to be complex (64,66), it cannot be excluded that the very intensive spot, as it is seen in the *N*-OH-2-AAF-treated samples, is a mixture of several different DNA adducts.

After a single 3 h treatment with 2-AAF at doses of 50 and 150 µg/cm² 2-AAF-derived adducts were minimal, but detectable, whereas no 2-AAF-related adducts were present in the SC. After three treatments with 2-AAF over 48 h clearly elevated levels of up to ~10 adducts per 10^8 nucleotides were observed (Figure 5a, b and f). Application of the three-treatment protocol with 2-AAF at 150 µg/cm² in the presence of APC resulted in an additional, but non-significant increase in DNA adduct levels (Figure 5b and f). As expected, a single 3 h exposure to the reactive metabolites *N*-OH-2-AAF and *N*-OH-2-AF resulted in massive increases in DNA adduct formation with levels being at least 10–100-fold greater than those observed with 2-AAF after multiple exposures (Figure 5c, d and g). Three treatments with BaP, used as PC, at a dose of 12.5 µg/cm² over 48 h induced adduct levels of ~50 adducts per 10^8 nucleotides in the Phenion®FT skin tissues, with levels also slightly, but non-significantly augmented in the presence of APC (Figure 5e and h). One single adduct spot was detected after BaP exposure, which was previously identified as 10-(deoxyguanosin-N^2-yl)-7,8,9-trihydroxy-7,8,9,10-tetrahydro-BaP (dG-N^2-BPDE) (62).

Discussion

The Phenion®FT (epidermal and dermal layers) and EpiDerm™ (epidermis only) 3D reconstructed skin tissue models are composed of primary and p53 competent cells of human origin which maintains normal cell cycle control and DNA-repair competence (70,71).

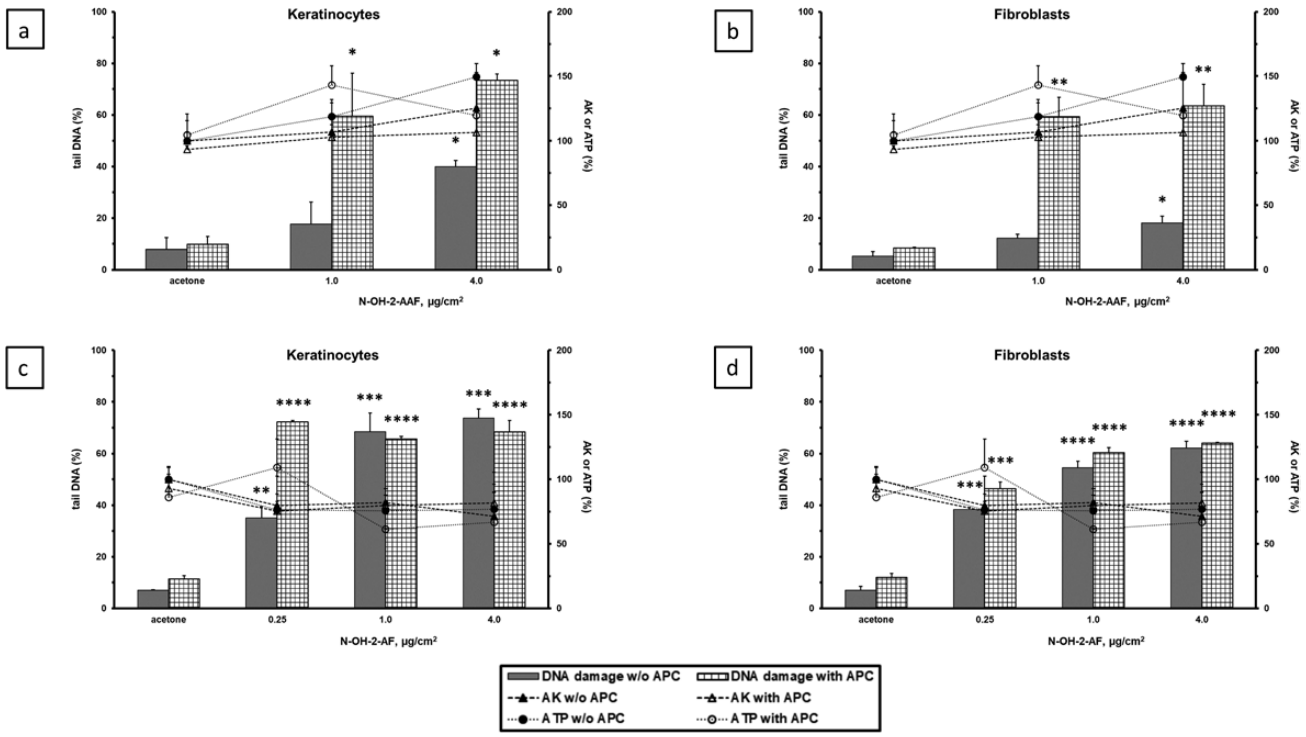

Fig. 4. DNA damage (% tail DNA) measured in the comet assay in the Phenion® FT skin model induced by *N*-OH-2-AAF (a, b, upper panels) or *N*-OH-2-AF (c, d, lower panels) ± APC in keratinocytes (a, c, left panels) and fibroblasts (b, d, right panels). Tissues were treated one time for 3 h ± APC. Cytotoxicity measures were % AK release and % ATP content relative to the solvent controls which were set at 100%. All values ($n = 3$) are mean ± SD. *$P < 0.05$, **$P < 0.01$, ***$P < 0.001$, ****$P < 0.0001$.

These skin models also have comparable phenotypical characteristics, gene and protein expression patterns, and activity levels for enzymes involved in xenobiotic metabolism as native human skin (11,14,17–23). Together, these characteristics make the 3D skin tissues a more representative model for testing the genotoxicity potential of dermally applied chemicals without the need for using exogenous metabolic enzyme systems and help to reduce the number of misleading genotoxic positive chemicals. Because the RSMN assay requires dividing cells, the EpiDerm™ skin model was chosen for the validation project efforts due to a higher rate of cell division than that seen in full-thickness reconstructed skin models (unpublished observations) and a low-background level of DNA damage in the RSMN (2,3). The original 3D skin comet assay validation work was also conducted in the EpiDerm™ skin model (1). However, since a significant number of experiments were invalid due to high-background levels of DNA damage, subsequent validation efforts for the skin comet assay were shifted to full-thickness skin models which were shown to have lower and less variable background DNA damage levels in the skin comet assay (4).

The comet assay detects a wide range of genotoxic damage including both chromosomal damage and DNA lesions that may result in gene mutations whereas the micronucleus assay detects only chromosomal damage caused by clastogens and aneugens. 2-AAF is primarily a mutagen, but also shows positive responses in clastogenicity tests *in vivo* in and *in vitro* after metabolic activation (34,46,47,72,73). The skin comet and RSMN assays were validated for topically applied chemicals in 3D reconstructed human skin models through the testing of various classes of chemicals with known genotoxic and non-genotoxic profiles *in vivo*, including promutagens that are not genotoxic themselves but can be converted into mutagenic metabolites. The original protocols for both the skin comet and RSMN assays were further optimised to include additional treatments and extended treatment times to increase their sensitivity for detecting chemicals that only show weak genotoxicity after skin exposure (e.g. diethylstilbestriol) as well as promutagens (e.g. BaP) without decreasing the specificity of the assays (4,53). These modifications were necessary for detecting promutagens since the basal expression levels of various xenobiotic-metabolising enzymes in human skin and 3D reconstructed human skin models, especially phase I enzymes (e.g. CYP1A family members) often involved in the activation of xenobiotics, are usually very low but are inducible after multiple exposures to these chemicals (18,20,21,74).

For 2-AAF, generation of the ultimate DNA-reactive compounds requires further phase II metabolism of *N*-OH-2-AAF or *N*-OH-2-AF by sulphation or *O*-acetylation (34–36,38,42–44). NAT2, which has been shown to have an important role in the *O*-acetylation of *N*-OH-2-AF in the liver and other tissues (75), is not detectable in native human skin and reconstructed human skin tissue models (20). NAT1 expression, however, is readily measurable in native skin and skin tissue models and NAT1 can also catalyse the same bioactivation step for 2-AAF (17,44,75). The need for induction of CYP1A and/or lack of NAT2 in skin is a possible explanation for the relatively lower genotoxic and carcinogenic effects of 2-AAF in the skin compared to liver and other tissues. However, the large response seen to a single acute 3 h exposure *N*-OH-2-AAF and *N*-OH-2-AF in the skin comet assay suggests that the sulphation or *O*-acetylation activity in skin is sufficient for the final bioactivation of 2-AAF once the *N*-hydroxylated metabolites are present.

Since the responses to 2-AAF, *N*-OH-2-AAF and *N*-OH-2-AF in both the standard and optimised versions of the skin comet and RSMN assays showed a low-sensitivity in the RSMN, the number of treatments was therefore increased from two (over 48 h) to three

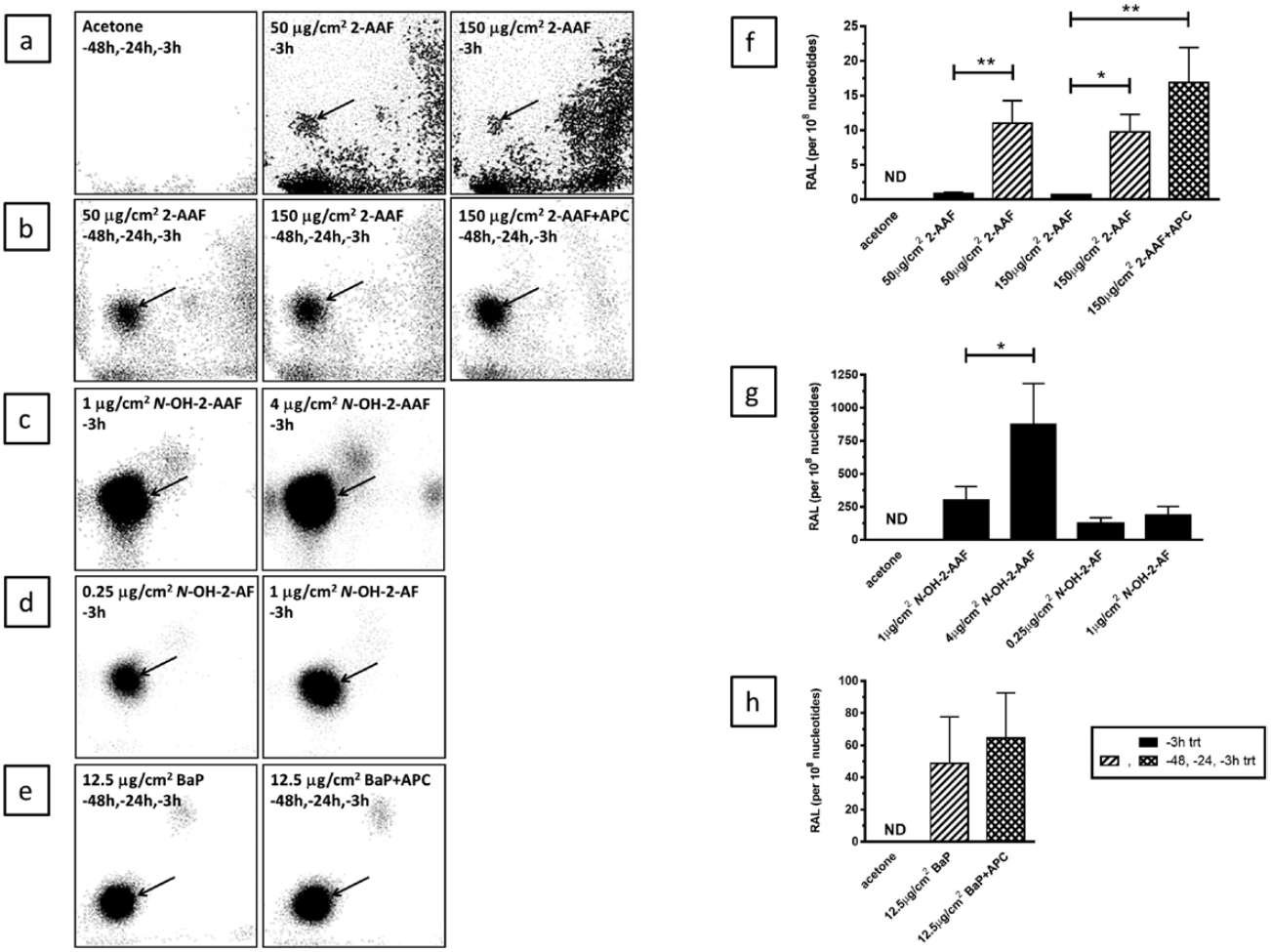

Fig. 5. DNA adducts in the Phenion® FT skin model. Tissues were treated three times (48, 24 and 3 h) with 2-AAF or BaP ± APC or 1 time (3 h) with 2-AAF, *N*-OH-2-AAF or *N*-OH-2-AAF (see figure legends for treatment times). The left panels (a–e) are representative autoradiographic profiles of the DNA adducts formed in Phenion®FT skin tissues after exposure. The origins, at the bottom left-hand corners on the TLC plates, were cut off before imaging and the arrows indicate the adduct spots used in the quantitation of the adduct levels shown in the graphs in the right panels (f–h). All values ($n = 3$) are mean ± SD. DNA adduct levels are calculated per 10^8 normal nucleotides. $^*P < 0.05$, $^{**}P < 0.01$. *P* values for specific group comparisons are shown within brackets. No statistical comparisons to the SC group were done as 2-AAF-related DNA adducts in the controls were not detectable (ND). PC: BaP. Note: the adduct spots found from exposure to 2-AAF, *N*-OH-2-AAF or *N*-OH-2-AF are not distinguishable on TLC.

exposures (over 72 h) at 24 h intervals. However, even with the optimised protocol for the RSMN assay, the response to 2-AAF was still not significant when tested after three treatments up to the highest possible concentration limited by cytotoxicity (Figure 2b and S. Pfuhler et. al., in preparation). Further, the weak responses seen after multiple direct exposures to two known genotoxic 2-AAF metabolites in the RSMN demonstrates that likely insufficient levels of the DNA reactive intermediates are formed after 2-AAF treatment to induce a detectable clastogenic response in the RSMN. A significant response in the RSMN was only measurable after three exposures to the highly reactive *N*-OH-2-AF metabolite, but not to *N*-OH-2-AAF. In support of these results, dermal application of 2-AAF in mice resulted in the formation of both dG-C8-AF and dG-N^2-AAF DNA adducts in skin, with dG-C8-AF being the predominant adduct (51), although *N*-OH-2-AAF can also be metabolised to form dG-C8-AF.

In the optimised protocol for the skin comet assay, the number of treatments was increased from one (3 h) to three exposures (over 48 h). In addition, APC was employed 1 h prior to the final chemical treatment. Inhibiting the DNA repair function of polymerases α and δ (54) likely also amplified the single strand breaks generated during excision repair resulting in increased comet formation without significantly affecting basal DNA damage as shown previously (4). The protocol optimised in this way resulted in a small, but statistically significant and reproducible response after multiple exposures to 2-AAF in the APC-modified skin comet assay. These results are also supported by the finding of another laboratory in the 3D skin comet assay validation project work which tested 2-AAF under double-blinded conditions and found a positive response in a similar dose range only in the APC-modified comet assay (S. Pfuhler et. al., submitted). Further, using a direct measure of DNA binding, treatment with 2-AAF led to a significant increase in the levels of bulky DNA adducts after multiple exposures compared to those seen after a single 3 h treatment which is likely due to the induction of xenobiotic-metabolising enzymes after repeated 2-AAF treatment.

Direct application of two DNA reactive metabolites of 2-AAF further demonstrated the increased sensitivity of the skin comet assay compared to the RSMN assay to the type of DNA damage caused by 2-AAF. A single 3 h treatment of the Phenion®FT skin tissues with both *N*-OH-2-AAF or *N*-OH-2-AF induced a highly

significant increase in the DNA damage in the skin comet assay in both keratinocytes and fibroblasts as well as a strong increase in the level of DNA adducts. The DNA strand breaks comet induced by a single treatment with *N*-OH-2-AAF or *N*-OH-2-AF were further amplified to maximal levels in the presence of APC.

Interestingly, although *N*-OH 2-AF was more potent in the skin comet assay than *N*-OH-2-AAF, the level of DNA adducts measured in response to a single 3 h treatment with *N*-OH-2-AF were not significantly different to those observed after exposure to *N*-OH-2-AAF when testing the same dose (1 µg/cm^2). The reason for this discrepancy is unknown, but DNA lesions detected by the comet assay (strand breaks) are different than those detected by ^{32}P-postlabelling (DNA adducts). Thus, it is possible that the potency in terms of DNA damage for *N*-OH-2-AF is different in both assays. One possible explanation is that the *N*-OH-2-AF-derived DNA adducts are more potent inducers of DNA strand breaks than the *N*-OH-2-AAF-derived DNA adducts, although dG-C8-AF is assumed to be the major adduct formed after treatment with both *N*-OH-2-AF and *N*-OH-2-AAF. However, ^{32}P-postlabelling does not allow direct structural identification of the DNA adducts formed (59,60) and 2-AAF has been shown to be capable of forming multiple adducts which can be labelled with different efficiency during ^{32}P-postlabelling (66,68). Differences in the short- and long-term persistence of 2-AAF-induced DNA adducts have been reported (64,68,76). Thus, it can be speculated that the individual adducts formed (i.e. dG-C8-AF, dG-C8-AAF and dG-*N*^{2}-AAF) may have different potencies to induce DNA adducts breaks or may show differences in DNA repair (77) thereby modulating the formation of 'repair-induced' nicks in the DNA which could generate a greater amount of detectable damage in the comet assay when treating with *N*-OH-2-AF compared to *N*-OH-2-AAF. Thus, full structural characterisation of the DNA adducts induced by 2-AAF, *N*-OH-2-AAF and *N*-OH-2-AF in the 3D reconstructed human skin models and the kinetics of those adducts could help to clarify this phenomenon and be the focus of future studies.

In summary, our results suggest that enzyme(s) involved in 2-AAF metabolism can be induced in human skin tissue models. Measurement of the DNA adducts which are a direct measure of DNA binding of reactive intermediates formed during bioactivation, clearly showed that multiple treatments with 2-AAF resulted in increased levels of DNA adducts indicating that enzyme(s) involved in 2-AAF bioactivation can be induced in the Phenion®FT skin model. In the presence of the DNA repair inhibitor, APC, DNA adduct levels remained elevated and a weak, but statistically significant and reproducible increase in DNA damage was observed in the skin comet assay. Together, these results support the use of the APC-modified extended treatment protocol for increasing the sensitivity of the skin comet assay for detecting xenobiotics such as 2-AAF that require metabolic activation to be converted to genotoxic DNA reactive compounds. Our results also demonstrate that the type of DNA damage caused by 2-AAF metabolites is more efficiently detected in the skin comet assay than in the RSMN assay.

Acknowledgements

The authors would like to thank Cathy Lester for her valuable contribution to preparation of the 2-AAF metabolism figure for this manuscript. Work at King's College London was supported by the National Institute for Health Research Health Protection Research Unit (NIHR HPRU) in Health Impact of Environmental Hazards at King's College London in partnership with Public Health England (PHE) and Imperial College London. The views expressed in this article are those of the authors and not necessarily those of the National Health Service, the National Institute for Health Research, the Department of Health and Social Care or Public Health England.
Conflict of interest statement: None declared.

References

1. Reus, A. A., Reisinger, K., Downs, T. R., Carr, G. J., Zeller, A., Corvi, R., Krul, C. A. and Pfuhler, S. (2013) Comet assay in reconstructed 3D human epidermal skin models–investigation of intra- and inter-laboratory reproducibility with coded chemicals. *Mutagenesis*, 28, 709–720.
2. Curren, R. D., Mun, G. C., Gibson, D. P. and Aardema, M. J. (2006) Development of a method for assessing micronucleus induction in a 3D human skin model (EpiDerm). *Mutat. Res.*, 607, 192–204.
3. Dahl, E. L., Curren, R., Barnett, B. C., *et al.* (2011) The reconstructed skin micronucleus assay (RSMN) in EpiDerm™: detailed protocol and harmonized scoring atlas. *Mutat. Res.*, 720, 42–52.
4. Reisinger, K., Blatz, V., Brinkmann, J., *et al.* (2018) Validation of the 3D Skin Comet assay using full thickness skin models: transferability and reproducibility. *Mutat. Res. Genet. Toxicol. Environ. Mutagen.*, 827, 27–41.
5. EU. (2009) European Union Regulation (EC) No. 1223/2009 of the European Parliament and of the Council of 30 November 2009 on cosmetic products (recast). *Off. J. Eur. Union*, L342, 59–209.
6. Pfuhler, S., Kirst, A., Aardema, M., *et al.* (2010) A tiered approach to the use of alternatives to animal testing for the safety assessment of cosmetics: genotoxicity. A COLIPA analysis. *Regul. Toxicol. Pharmacol.*, 57, 315–324.
7. Pfuhler, S., Fautz, R., Ouedraogo, G., *et al.* (2014) The Cosmetics Europe strategy for animal-free genotoxicity testing: project status up-date. *Toxicol. In Vitro*, 28, 18–23.
8. Kirkland, D., Aardema, M., Henderson, L. and Müller, L. (2005) Evaluation of the ability of a battery of three in vitro genotoxicity tests to discriminate rodent carcinogens and non-carcinogens. I. Sensitivity, specificity and relative predictivity. *Mutat. Res.*, 584, 1–256.
9. Pfuhler, S., Fellows, M., van Benthem, J., *et al.* (2011) In vitro genotoxicity test approaches with better predictivity: summary of an IWGT workshop. *Mutat. Res.*, 723, 101–107.
10. Ahmad, N. and Mukhtar, H. (2004) Cytochrome p450: a target for drug development for skin diseases. *J. Invest. Dermatol.*, 123, 417–425.
11. Oesch, F., Fabian, E. and Landsiedel, R. (2018) Xenobiotica-metabolizing enzymes in the skin of rat, mouse, pig, guinea pig, man, and in human skin models. *Arch. Toxicol.*, 92, 2411–2456.
12. Oesch, F., Fabian, E., Oesch-Bartlomowicz, B., Werner, C. and Landsiedel, R. (2007) Drug-metabolizing enzymes in the skin of man, rat, and pig. *Drug Metab. Rev.*, 39, 659–698.
13. Zeller, A. and Pfuhler, S. (2014) N-acetylation of three aromatic amine hair dye precursor molecules eliminates their genotoxic potential. *Mutagenesis*, 29, 37–48.
14. Brinkmann, J., Stolpmann, K., Trappe, S., *et al.* (2013) Metabolically competent human skin models: activation and genotoxicity of benzo[*a*]pyrene. *Toxicol. Sci.*, 131, 351–359.
15. Lademann, J., Richter, H., Jacobi, U., *et al.* (2008) Human percutaneous absorption of a direct hair dye comparing in vitro and in vivo results: implications for safety assessment and animal testing. *Food Chem. Toxicol.*, 46, 2214–2223.
16. Hu, T., Bailey, R. E., Morrall, S. W., Aardema, M. J., Stanley, L. A. and Skare, J. A. (2009) Dermal penetration and metabolism of p-aminophenol and p-phenylenediamine: application of the EpiDerm human reconstructed epidermis model. *Toxicol. Lett.*, 188, 119–129.
17. Wiegand, C., Hewitt, N. J., Merk, H. F. and Reisinger, K. (2014) Dermal xenobiotic metabolism: a comparison between native human skin, four in vitro skin test systems and a liver system. *Skin Pharmacol. Physiol.*, 27, 263–275.
18. Götz, C., Pfeiffer, R., Tigges, J., *et al.* (2012) Xenobiotic metabolism capacities of human skin in comparison with a 3D epidermis model and keratinocyte-based cell culture as in vitro alternatives for chemical testing: activating enzymes (Phase I). *Exp. Dermatol.*, 21, 358–363.

19. Götz, C., Pfeiffer, R., Tigges, J., *et al*. (2012) Xenobiotic metabolism capacities of human skin in comparison with a 3D-epidermis model and keratinocyte-based cell culture as in vitro alternatives for chemical testing: phase II enzymes. *Exp. Dermatol.*, 21, 364–369.
20. Hu, T., Khambatta, Z. S., Hayden, P. J., *et al*. (2010) Xenobiotic metabolism gene expression in the EpiDermin vitro 3D human epidermis model compared to human skin. *Toxicol. In Vitro*, 24, 1450–1463.
21. Hewitt, N. J., Edwards, R. J., Fritsche, E., *et al*. (2013) Use of human in vitro skin models for accurate and ethical risk assessment: metabolic considerations. *Toxicol. Sci.*, 133, 209–217.
22. Gibbs, S., van de Sandt, J. J., Merk, H. F., Lockley, D. J., Pendlington, R. U. and Pease, C. K. (2007) Xenobiotic metabolism in human skin and 3D human skin reconstructs: a review. *Curr. Drug Metab.*, 8, 758–772.
23. Jäckh, C., Blatz, V., Fabian, E., Guth, K., van Ravenzwaay, B., Reisinger, K. and Landsiedel, R. (2011) Characterization of enzyme activities of Cytochrome P450 enzymes, Flavin-dependent monooxygenases, N-acetyltransferases and UDP-glucuronyltransferases in human reconstructed epidermis and full-thickness skin models. *Toxicol. In Vitro*, 25, 1209–1214.
24. Wilson, R. H., DeEds, F., and Cox, A. J. (1941) The toxicity and carcinogenic activity of 2-acetaminofluorene. *Cancer Res.*, 1, 595–608.
25. Morris, H. P., Dubnik, C. S. and Johnson, J. M. (1950) Studies of the carcinogenic action in the rat of 2-nitro, 2-amino-, 2-acetylamino-, and 2-diacetylaminofluorene after ingestion and after painting. *J. Natl. Cancer Inst.*, 10, 1201–1213.
26. Bielschowski, F. (1944) Distant tumours produced by 2-amino- and 2-acetyl-amino-fluorene. *Br. J. Exp. Pathol.*, 25, 1–4.1.
27. OEHHA (1998) *Evidence on the Carcinogenicity of 2-Aminofluorene*. pp. 1–18. https://oehha.ca.gov/media/downloads/proposition-65/chemicals/hid2amin.pdf (for the document) or https://oehha.ca.gov/ (for the web-site)
28. Goodall, C. M. (1966) Hepatic carcinogenesis in thyroidectomized rats: apparent blockade at the stage of initiation. *Cancer Res.*, 26, 1880–1883.
29. Miller, E. C., Miller, J. A. and Enomoto, M. (1964) The comparative carcinogenicities of 2-acetylaminofluorene and its n-hydroxy metabolite in mice, hamsters, and guinea pigs. *Cancer Res.*, 24, 2018–2031.
30. Miller, J. A., Sandin, R. B., Miller, E. C. and Rusch, H. P. (1955) The carcinogenicity of compounds related to 2-acetylaminofluorene. II. Variations in the bridges and the 2-substituent. *Cancer Res.*, 15, 188–199.
31. Bielschowsky, F. (1946) The carcinogenic action of 2-acetylaminofluorene and related compounds. *Br. Med. Bull.*, 4, 382–385.
32. Bielschowsky, F. and Bielschowsky, M. (1960) Carcinogenesis in the pituitary dwarf mouse. The response to 2-aminofluorene. *Br. J. Cancer*, 14, 195–199.
33. Ritchie, A. C. and Saffiotti, U. (1955) Orally administered 2-acetylaminofluorene as an initiator and as a promoter in epidermal carcinogenesis in the mouse. *Cancer Res.*, 15, 84–88.
34. Heflich, R. H. and Neft, R. E. (1994) Genetic toxicity of 2-acetylaminofluorene, 2-aminofluorene and some of their metabolites and model metabolites. *Mutat. Res.*, 318, 73–114.
35. Weisburger, E. K. and Weisburger, J. H. (1958) Chemistry, carcinogenicity, and metabolism of 2-fluorenamine and related compounds. *Adv. Cancer Res.*, 5, 331–431.
36. Kriek, E. (1992) Fifty years of research on N-acetyl-2-aminofluorene, one of the most versatile compounds in experimental cancer research. *J. Cancer Res. Clin. Oncol.*, 118, 481–489.
37. Weisburger, E. K., Grantham, P. H. and Weisburger, J. H. (1964) Differences in the metabolism of n-hydroxy-n-2-fluorenylacetamide in male and female rats. *Biochemistry*, 3, 808–812.
38. Verna, L., Whysner, J. and Williams, G. M. (1996) 2-Acetylaminofluorene mechanistic data and risk assessment: DNA reactivity, enhanced cell proliferation and tumor initiation. *Pharmacol. Ther.*, 71, 83–105.
39. Cramer, J. W., Miller, J. A. and Miller, E. C. (1960) N-hydroxylation: a new metabolic reaction observed in the rat with the carcinogen 2-acetylaminofluorene. *J. Biol. Chem.*, 235, 885–888.
40. Miller, E. C., Miller, J. A. and Hartmann, H. A. (1961) N-hydroxy-2-acetylaminofluorene: a metabolite of 2-acetylaminofluorene with increased carcinogenic activity in the rat. *Cancer Res.*, 21, 815–824.
41. Goodall, C. M. and Gasteyer, S. (1966) Skin tumours and sarcomata induced in rats by N-hydroxy-2-acetylaminofluorene. *Nature*, 211, 1422.
42. Rudo, K., Meyers, W. C., Dauterman, W. and Langenbach, R. (1987) Comparison of human and rat hepatocyte metabolism and mutagenic activation of 2-acetylaminofluorene. *Cancer Res.*, 47, 5861–5867.
43. Rodrigues, A. S., Silva, I. D., Caria, M. H., Laires, A., Chaveca, T., Glatt, H. R. and Rueff, J. (1994) Genotoxicity assessment of aromatic amines and amides in genetically engineered V79 cells. *Mutat. Res.*, 341, 93–100.
44. Rendic, S. and Guengerich, F. P. (2012) Contributions of human enzymes in carcinogen metabolism. *Chem. Res. Toxicol.*, 25, 1316–1383.
45. Razzouk, C., Batardy-Grégoire, M. and Roberfroid, M. (1982) Metabolism of N-hydroxy-2-acetylaminofluorene and N-hydroxy-2-aminofluorene by guinea pig liver microsomes. *Cancer Res.*, 42, 4712–4718.
46. TOXNET. (2019) *2-Acetylaminofluorene*. https://toxnet.nlm.nih.gov/newtoxnet/index.html (for the web-site)
47. NTP. (2019) *National Toxicology Program: Testing Status of 2-Acetylaminofluorene 10361-C*. https://ntp.niehs.nih.gov/publications/index.html (for the web-site)
48. Langenbach, R. and Rudo, K. (1988) Human hepatocyte and kidney cell metabolism of 2-acetylaminofluorene and comparison to the respective rat cells. *Cell Biol. Toxicol.*, 4, 453–465.
49. Langenbach, R., Rudo, K., Ellis, S., Hix, C. and Nesnow, S. (1987) Species variation in bladder cell and liver cell activation of acetylaminofluorene. *Cell Biol. Toxicol.*, 3, 303–319.
50. Géniès, C., Jamin, E. L., Debrauwer, L., *et al*. (2019) Comparison of the metabolism of 10 chemicals in human and pig skin explants. *J. Appl. Toxicol.*, 39, 385–397.
51. Schurdak, M. E. and Randerath, K. (1989) Effects of route of administration on tissue distribution of DNA adducts in mice: comparison of 7H-dibenzo(c,g)carbazole, benzo(a)pyrene, and 2-acetylaminofluorene. *Cancer Res.*, 49, 2633–2638.
52. Gutmann, H. R. and Peters, J. H. (1957) The fate of 2-acetylaminofluorene and 2-amino-fluorene after application to rat skin. *Cancer Res.*, 17, 167–176.
53. Aardema, M. J., Barnett, B. B., Mun, G. C., Dahl, E. L., Curren, R. D., Hewitt, N. J. and Pfuhler, S. (2013) Evaluation of chemicals requiring metabolic activation in the EpiDerm™ 3D human reconstructed skin micronucleus (RSMN) assay. *Mutat. Res.*, 750, 40–49.
54. Speit, G., Schütz, P. and Hoffmann, H. (2004) Enhancement of genotoxic effects in the comet assay with human blood samples by aphidicolin. *Toxicol. Lett.*, 153, 303–310.
55. Mun, G. C., Aardema, M. J., Hu, T., Barnett, B., Kaluzhny, Y., Klausner, M., Karetsky, V., Dahl, E. L. and Curren, R. D. (2009) Further development of the EpiDerm 3D reconstructed human skin micronucleus (RSMN) assay. *Mutat. Res.*, 673, 92–99.
56. OECD. (2016) *Guidelines for the Testing of Chemicals, Test No. 487: In Vitro Mammalian Cell Micronucleus Test*. Paris, France: OECD Publishing.
57. Olsson, T., Gulliksson, H., Palmeborn, M., Bergström, K. and Thore, A. (1983) Leakage of adenylate kinase from stored blood cells. *J. Appl. Biochem.*, 5, 437–445.
58. Kangas, L., Grönroos, M. and Nieminen, A. L. (1984) Bioluminescence of cellular ATP: a new method for evaluating cytotoxic agents in vitro. *Med. Biol.*, 62, 338–343.
59. Phillips, D. H. and Arlt, V. M. (2007) The 32P-postlabeling assay for DNA adducts. *Nat. Protoc.*, 2, 2772–2781.
60. Phillips, D. H. and Arlt, V. M. (2014) ^{32}P-postlabeling analysis of DNA adducts. *Methods Mol. Biol.*, 1105, 127–138.
61. Wohak, L. E., Baranski, A. C., Krais, A. M., Schmeiser, H. H., Phillips, D. H. and Arlt, V. M. (2018) The impact of p53 function on the metabolic activation of the carcinogenic air pollutant 3-nitrobenzanthrone and its metabolites 3-aminobenzanthrone and N-hydroxy-3-aminobenzanthrone in human cells. *Mutagenesis*, 33, 311–321.
62. Reed, L., Mrizova, I., Barta, F., *et al*. (2018) Cytochrome b 5 impacts on cytochrome P450-mediated metabolism of benzo[*a*]pyrene and its DNA adduct formation: studies in hepatic cytochrome b 5 /P450 reductase null (HBRN) mice. *Arch. Toxicol.*, 92, 1625–1638.

63. Dunnett, C.W. (1955) A multiple comparison procedure for comparing several treatments with a control AU – Dunnett, Charles W. *J. Am. Stat. Assoc.*, 50, 1096–1121.
64. Gupta, R. C. (1988) 32P-adduct assay: short- and long-term persistence of 2-acetylaminofluorene-DNA adducts and other applications of the assay. *Cell Biol. Toxicol.*, 4, 467–474.
65. Culp, S. J., Poirier, M. C. and Beland, F. A. (1993) Biphasic removal of DNA adducts in a repetitive DNA sequence after dietary administration of 2-acetylaminofluorene. *Environ. Health Perspect.*, 99, 273–275.
66. Möller, L. and Zeisig, M. (1993) DNA adduct formation after oral administration of 2-nitrofluorene and N-acetyl-2-aminofluorene, analyzed by 32P-TLC and 32P-HPLC. *Carcinogenesis*, 14, 53–59.
67. Chen, T., Mittelstaedt, R. A., Aidoo, A., Hamilton, L. P., Beland, F. A., Casciano, D. A. and Heflich, R. H. (2001) Comparison of hprt and lacI mutant frequency with DNA adduct formation in N-hydroxy-2-acetylaminofluorene-treated Big Blue rats. *Environ. Mol. Mutagen.*, 37, 195–202.
68. Williams, G. M., Duan, J. -D., Iatropoulos, M. J., and Kobets, T. (2015) A no observed adverse effect level for DNA adduct formation in rat liver with prolonged dosing of the hepatocarcinogen 2-acetylaminofluorene. *Toxicol. Res.*, 4, 233–240.
69. Williams, G. M., Duan, J. D., Iatropoulos, M. J. and Perrone, C. E. (2016) Sex differences in DNA damage produced by the carcinogen 2-acetylaminofluorene in cultured human hepatocytes compared to rat liver and cultured rat hepatocytes. *Arch. Toxicol.*, 90, 427–432.
70. Mewes, K. R., Raus, M., Bernd, A., Zöller, N. N., Sättler, A. and Graf, R. (2007) Elastin expression in a newly developed full-thickness skin equivalent. *Skin Pharmacol. Physiol.*, 20, 85–95.
71. Kubilus, J., Hayden, P. J., Ayehunie, S., Lamore, S. D., Servattalab, C., Bellavance, K. L., Sheasgreen, J. E. and Klausner, M. (2004) Full thickness EpiDerm: a dermal-epidermal skin model to study epithelial-mesenchymal interactions. *Altern. Lab. Anim.*, 32 (Suppl 1A), 75–82.
72. van de Poll, M.L., van der Hulst, D.A., Tates, A.D., and Meerman, J.H. (1990) Correlation between clastogenicity and promotion activity in liver carcinogenesis by N-hydroxy-2-acetylaminofluorene, N-hydroxy-4'-fluoro-4-acetylaminobiphenyl and N-hydroxy-4-acetylaminobiphenyl. *Carcinogenesis*, 11, 333–339.
73. van de Poll, M.L., van der Hulst, D.A., Tates, A.D., Mulder, G.J., and Meerman, J.H. (1989) The role of specific DNA adducts in the induction of micronuclei by N-hydroxy-2-acetylaminofluorene in rat liver in vivo. *Carcinogenesis*, 10, 717–722.
74. Götz, C., Hewitt, N. J., Jermann, E., Tigges, J., Kohne, Z., Hübenthal, U., Krutmann, J., Merk, H. F. and Fritsche, E. (2012) Effects of the genotoxic compounds, benzo[*a*]pyrene and cyclophosphamide on phase 1 and 2 activities in EpiDerm™ models. *Xenobiotica.*, 42, 526–537.
75. Hein, D. W., Doll, M. A., Rustan, T. D., Gray, K., Feng, Y., Ferguson, R. J. and Grant, D. M. (1993) Metabolic activation and deactivation of arylamine carcinogens by recombinant human NAT1 and polymorphic NAT2 acetyltransferases. *Carcinogenesis*, 14, 1633–1638.
76. Beland, F. A., Dooley, K. L. and Jackson, C. D. (1982) Persistence of DNA adducts in rat liver and kidney after multiple doses of the carcinogen N-hydroxy-2-acetylaminofluorene. *Cancer Res.*, 42, 1348–1354.
77. Mu, H., Kropachev, K., Wang, L., Zhang, L., Kolbanovskiy, A., Kolbanovskiy, M., Geacintov, N. E. and Broyde, S. (2012) Nucleotide excision repair of 2-acetylaminofluorene- and 2-aminofluorene-(C8)-guanine adducts: molecular dynamics simulations elucidate how lesion structure and base sequence context impact repair efficiencies. *Nucleic Acids Res.*, 40, 9675–9690.